



Ionosphere delay remote sensing during geomagnetic storms over Egypt using GPS phase observations

Ahmed Sedeek¹

Received: 7 May 2020 / Accepted: 30 July 2020 / Published online: 17 August 2020
© Saudi Society for Geosciences 2020

Abstract

Various factors can increase ionosphere activity, such as the geomagnetic latitude, altitude, and geomagnetic storms. These storms can result in a significant disruption of the Earth's atmosphere due to the interchange of solar wind energy into the milieu encompassing the Earth. The principal reason for this research is investigating the geomagnetic activity effect on ionospheric delays over Egypt using GPS (Global Positioning System) multi-frequency (L_2 and L_1) measurements. In this contribution, a GPS network spread over Egypt was utilized to figure ionosphere errors over Egypt, utilizing two models that rely upon GPS observable linear combination and smoothed phase observables. An algorithm was coded in MATLAB® environment and was called the Ionosphere Error Estimation (IEE) program. GPS phase observables were considered in this investigation to avoid blunders from pseudo-range measurements. Data from six ground-based multi-frequency GPS receivers located over Egypt have been chosen to study the impact of geomagnetic storms on ionospheric blunders. This paper presents the consequences of ionospheric blunders during disturbed and quiet days throughout the years of 2013 and 2014. Results clarify that the applied models using unsmoothed and smoothed phase observables show a good agreement in estimating ionospheric blunders, especially in quiet days. Ionospheric blunder standard deviation of mean (SDM) results from using smoothed phase observables that ranges from 16 to 3 cm in quiet conditions and ranges from 21 to 8 cm in stormy conditions. While ionospheric blunder SDM ranges from 17 to 5 cm in quiet days and from 23 to 8 cm in stormy days using unsmoothed phase observables. In The maximum ionosphere delay estimated over stormy days using the unsmoothed phase observables, its magnitude was 13.19 m at ASWN while the highest ionosphere error at ASWN station in quiet days was 6.83 m. In the maximum ionosphere delay estimated over stormy days using the smoothed phase observables, its magnitude was 13.34 m at ALAM while the highest ionosphere error at ALAM station in quiet days was 4.94 m. Finally, geomagnetic storms represent a real problem in equatorial and high-latitude zones, which causes a significant influence on the ionosphere blunder, and they have the capability of upsetting the results.

Keywords Ionosphere · Geomagnetic storm · Carrier phase · Remote sensing

Introduction

In GPS real-time applications, the obtained range from the satellite to the receiver is different from the true geometric range because of various provenance of blunders (Ghilani and Wolf 2014). The ionosphere causes a defer, which is a negative for phase observations and positive for the code ones

due to the total electron content (TEC) along the path from the GPS satellite to the receiver (Hofmann-Wellenhof et al. 2008). This postponement is viewed as the most fantastic provenance of all blunders that influence the GPS signals (Bhattacharya et al. 2008).

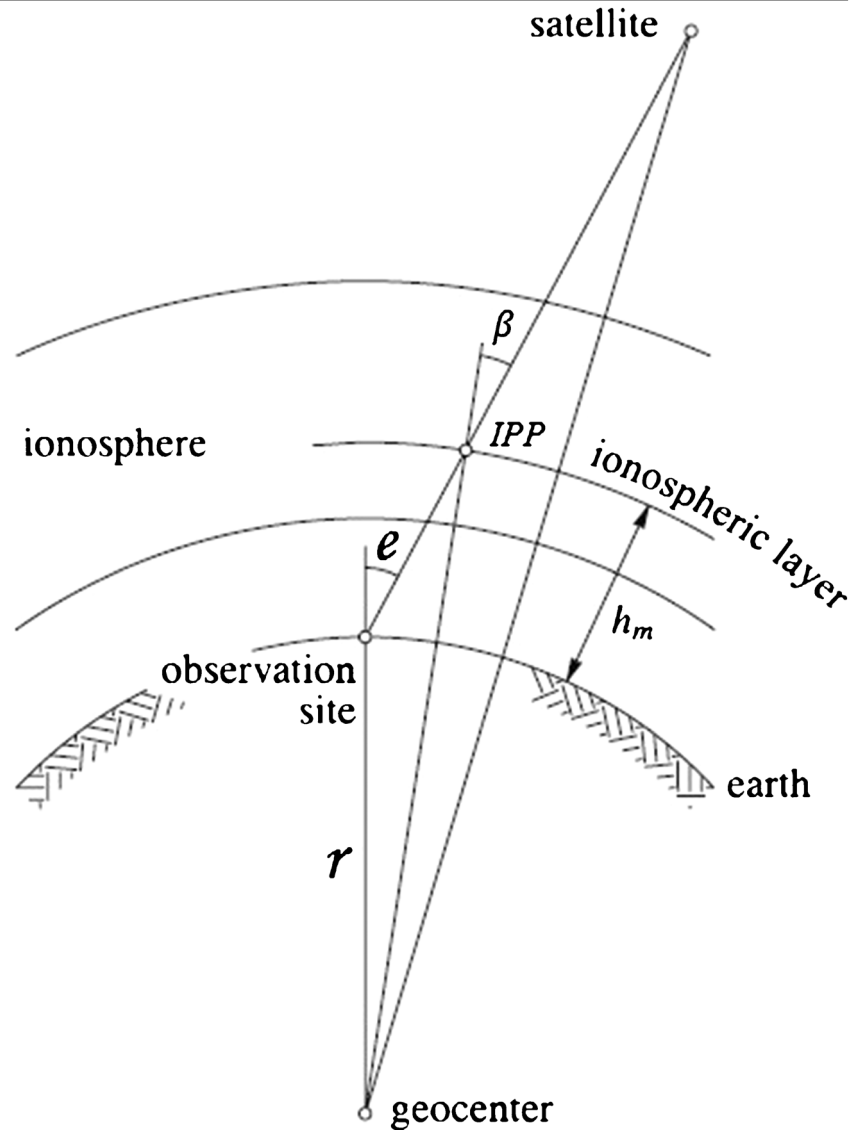
Moreover, the Sun plays a vital role in the magnitude of this error because the high solar activity that increases the amount of refraction induced by the ionosphere (Sickle 2015). A high energy wave known as solar wind is generated by the Sun. The solar wind reacts with the geomagnetic field, and occasionally, these charged particles rise significantly due to the solar flares on the surface of the Sun (Klobuchar 1991). Many particles arise in the atmosphere of the Sun, which is known as CMEs (coronal mass ejections). Many of such CMEs will significantly distort the Earth's magnetic field

Responsible Editor: Biswajeet Pradhan

✉ Ahmed Sedeek
eng.ahmedsedeek@gmail.com

¹ Higher Institute of Engineering and Technology, El-Behira, Egypt

Fig. 1 Elements of the ionospheric shell model (Hofmann-Wellenhof et al. 2008)



and induce a geomagnetic storm (Sidorov et al. 2019). Such storms that occur in northern auroral regions in particular and last many hours may often reach the middle and equatorial latitudes, disrupt the ionosphere, and degrade the performance of the GPS receiver (Sedeek et al. 2017; Elghazouly et al. 2019b; Elsayed et al. 2018).

The GPS signals travel from the space to the Earth passing through the ionosphere so that GPS signals considered as a sensor to estimate ionospheric delay. Although there are different agencies that provide global maps for ionospheric error in means of VTEC (vertical total electron content), these VTEC values over Egypt are interpolated because there is no IGS (International GNSS Service) GPS station over Egypt; so, the IEE MATLAB program developed to address GPS signals to estimate the ionospheric delay from a real data over Egypt.

The ionosphere products produced by the IGS analysis center uses pseudo-range observables to estimate the

ionospheric error because pseudo-range is free of an ambiguous term; so, it is easy to estimate ionosphere errors. As the phase observables are more accurate than the pseudo-range, a common approach is to smooth pseudo-range with the phase observables. The smoothed phase observables by pseudo-range eliminate noise and avoid addressing ambiguities directly (Xiang et al. 2017).

Since the consistency of estimated ionosphere errors depends mainly on the used observables, two approaches were considered in this contribution to compare and estimate ionospheric blunders using phase observables; the first one is using the linear combination to fix the ambiguity term after repairing cycle slips, the second approach smoothing pseudo-range with phase observables to avoid fixing ambiguity.

The objective of this contribution is to study remotely sensed ionospheric error using smoothed and unsmoothed phase observables during high and low geomagnetic activity over Egypt.

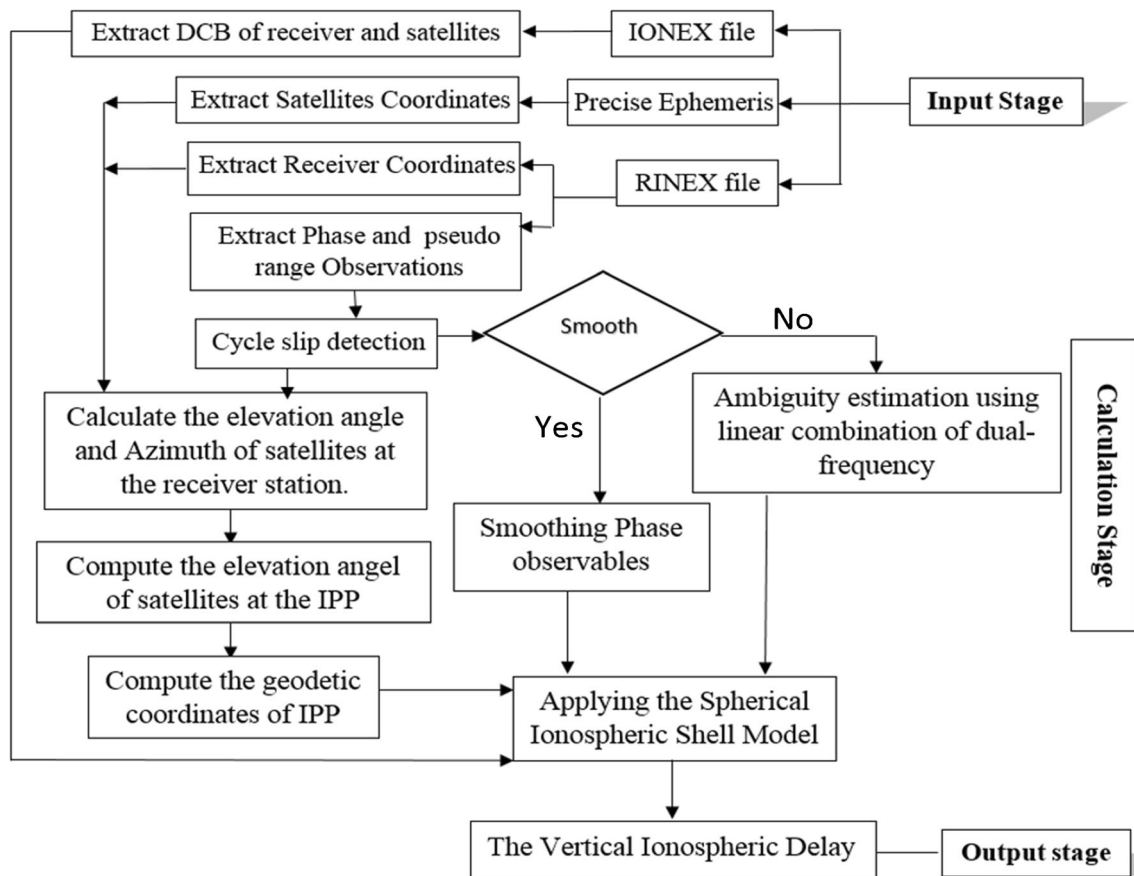


Fig. 2 Block diagram of the IEE program

The following sections are the applied mathematical algorithms, case study, results, and conclusion.

Ionosphere error estimation techniques

In this contribution, the geometric range between the receiver, satellite, and other frequency-independent errors was eliminated by combining phase (L_1-L_2) and pseudo-range (P_1-P_2) from GPS measurements. Ionosphere biases were estimated using phase observables by two different models, which were explained in the next section.

Melbourne-Wübbena linear combination of double-band phase and code observables utilized for distinguishing and repairing cycle slips in this current contribution. The cycle slip term $\Delta N_1(k) - \Delta N_2(k)$ when k is the epoch number can be estimated as (e.g., Dengynu et al. 2012; Elghazouly et al. 2019a):

$$\Delta N_1(k) - \Delta N_2(k) = N_{WL}(k-1) - N_{WL}(k) \tag{1}$$

Estimating ionosphere biases using phase observables

Fixing the ambiguities is essential to estimate ionospheric biases. In this model, phase observables were used without any smoothing (unsmoothed). The mathematical algorithm can be explicated as (e.g., Leandro 2009)

$$\begin{aligned} L_{GF} &= L_1 - L_2 \\ &= (1-\gamma)MF(I + \nabla_{\Phi}(\Phi_P - \Phi_0) + \nabla_{\lambda}(\lambda_P - \lambda_0)) \\ &\quad + Nb'_{gf} \end{aligned} \tag{2}$$

Table 1 G-scale and K_p index according to NOAA (<https://www.noaa.gov>)

G-scale	K_p	Storm activity	G-scale	K_p	Storm activity
G0	4 and lower	Below	G3	7	Strong
G1	5	Minor	G4	8	Severe
G2	6	Moderate	G5	9	Extreme

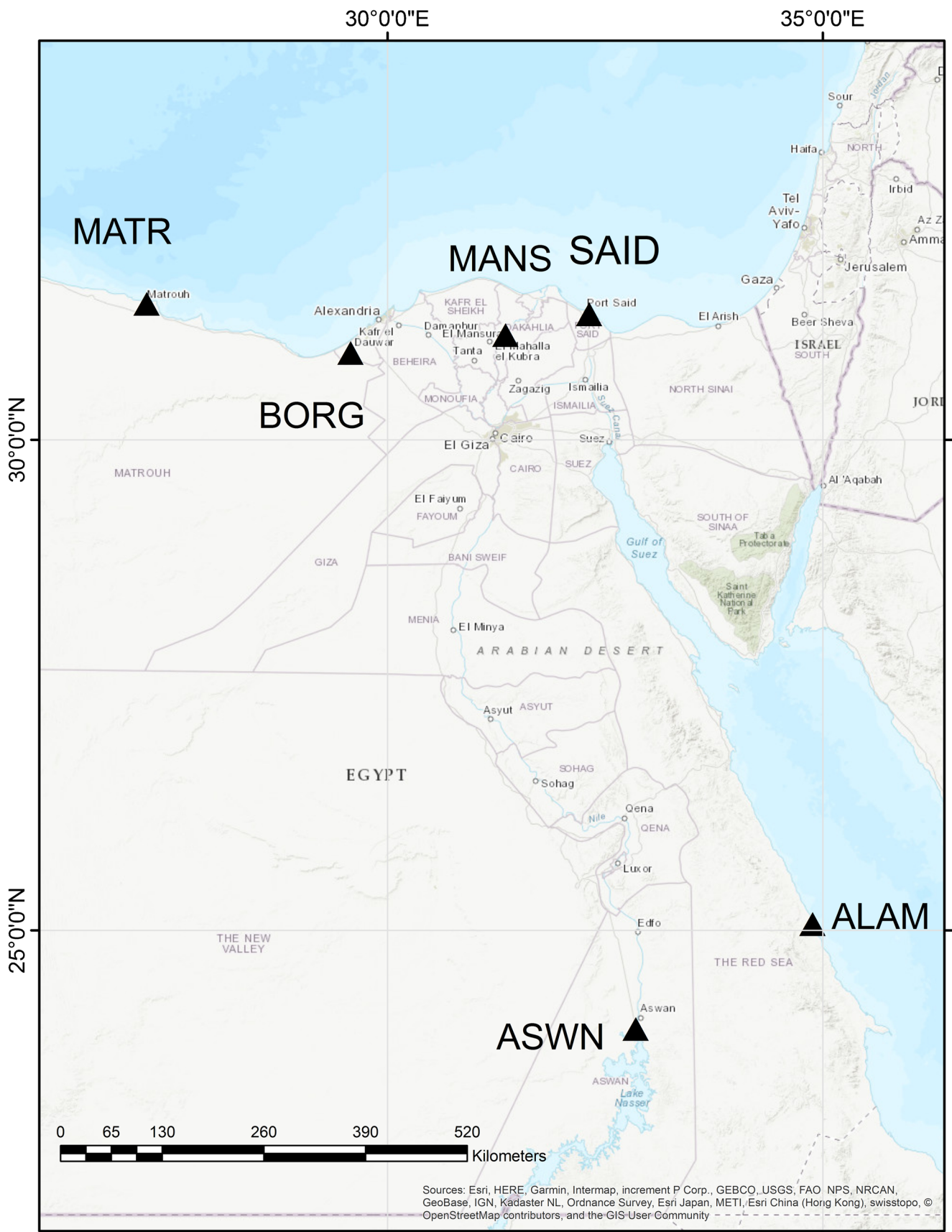


Fig. 3 Distribution of GNSS receivers over Egypt

Table 2 The geomagnetic storm activity during days of study (http://tesis.lebedev.ru/en/magnetic_storms.html/)

DOY	Days of quiet conditions			DOY	Days of stormy conditions		
	G-scale	Mean A_p	Mean K_p		G-scale	Mean A_p	Mean K_p
22, 2013	G0	4	0	76, 2013	G2	46	6
37, 2013	G0	2	1	50, 2014	G2	51	6
75, 2013	G0	15	3	51, 2014	G2	47	6
79, 2013	G0	9	3	52, 2014	G1	39	5

where L_{GF} is the geometry-free carrier-phase observation in length units, MF is the ionosphere mapping function expressed as Eq. (8), I is the vertical ionospheric delay at the station position, ∇_Φ and ∇_λ are the latitudinal and longitudinal gradients, respectively, Φ_p and λ_p are the geodetic latitude and longitude of the ionospheric piercing point, Φ_0 and λ_0 are the geodetic latitude and longitude of the station, γ is the factor to convert the ionospheric delay from L_1 to L_2 frequency, unitless and Nb'_{gf} is the ambiguity parameter which includes the carrier-phase integer ambiguity plus a collection of biases.

In this model, a combination of dual-frequency carrier phase and code data is used to estimate the ambiguity terms after repairing cycle slips using the following form (Xu 2007)

$$\begin{pmatrix} \lambda_1 N_1 \\ \lambda_2 N_2 \\ B_1 \\ C_p \end{pmatrix} = \begin{pmatrix} 1-2a & -2b \\ -2a & 2a-1 \\ 1/q & 0 \\ a & -1/qb \end{pmatrix} \begin{pmatrix} P_1 \\ P_2 \\ \lambda_1 \Phi_1 \\ \lambda_2 \Phi_2 \end{pmatrix} \quad (3)$$

where a is the geometry term and b is the ionosphere term, N_1 and N_2 are the unknown integer ambiguity of L_1 and L_2 ,

Fig. 4 Errors caused by the ionosphere at ALAM GPS station during stormy days (a) and quiet days (b)

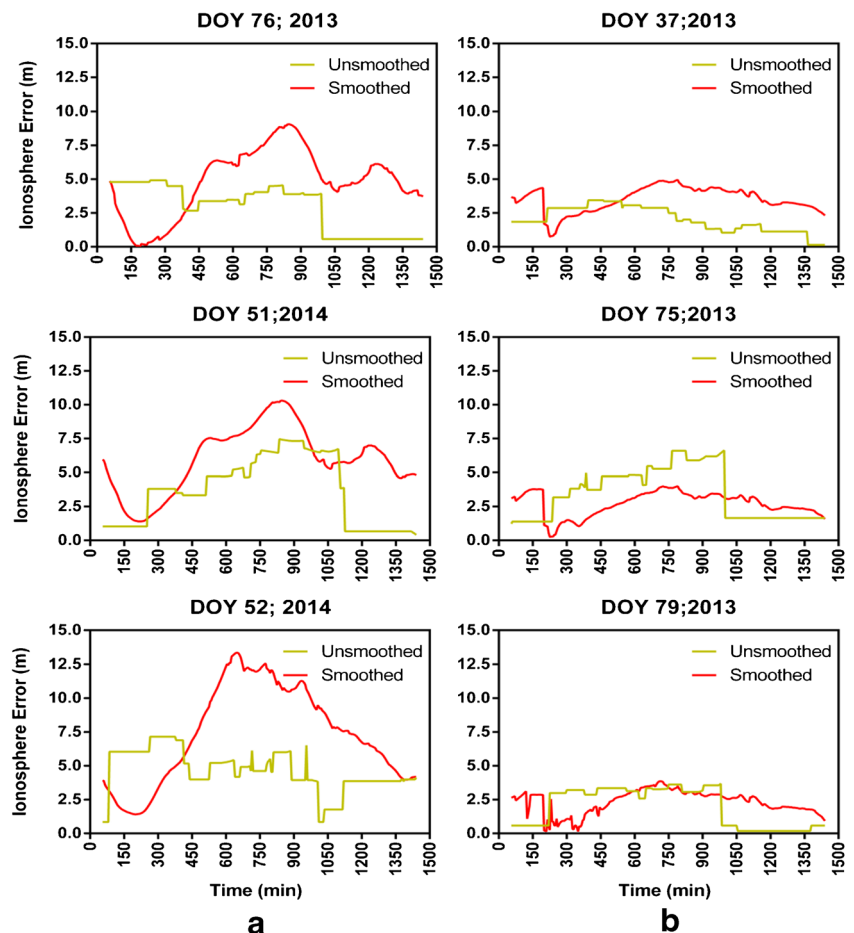
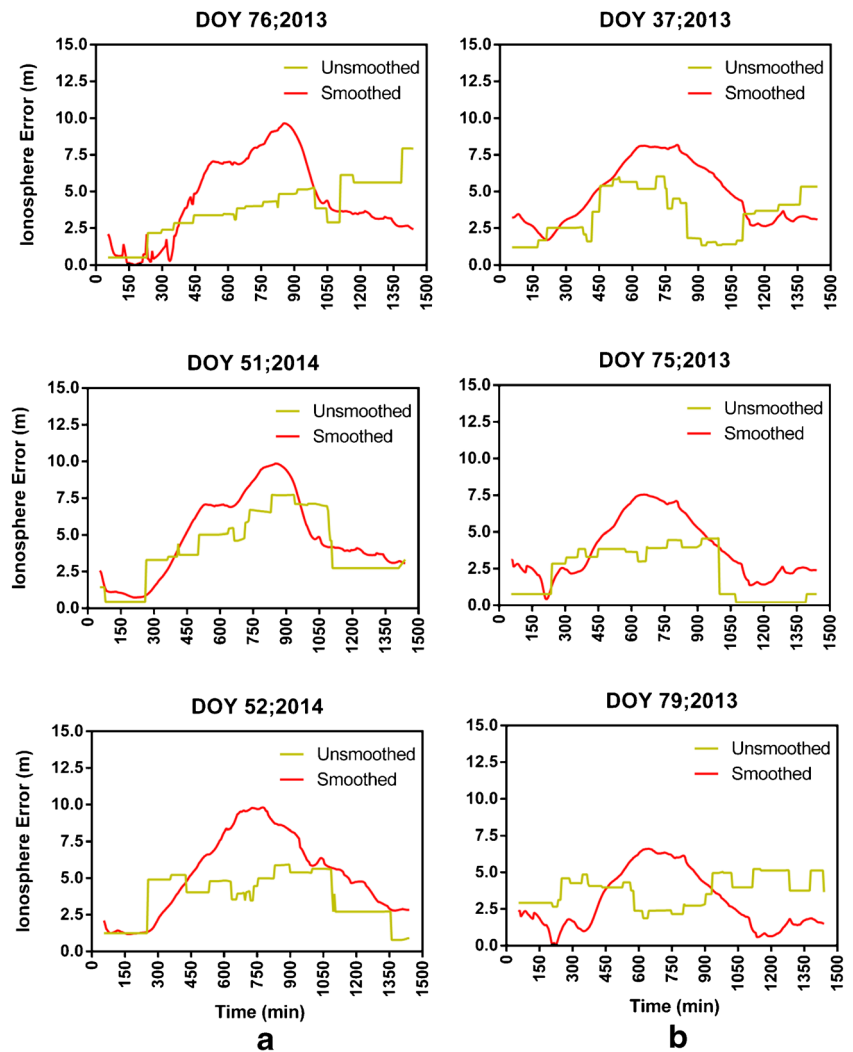


Fig. 5 Errors caused by the ionosphere at BORG GPS station during stormy days (a) and quiet days (b)



respectively, P_1 and P_2 are the observed pseudo-range on L_1 and L_2 , respectively, $q = (1/b)$, and ionosphere B_1 and geometry C_p are the functions of the codes and are independent on the phases. Sequential least square adjustment (SLSA) was applied to fix the ambiguity term using Eq. (10).

Estimating ionosphere biases using smoothed phase observables

The smoothing process used historically to estimate the ionospheric biases. The following steps can be defined as the corresponding ionospheric bias estimation process.

- 1- Cycle slip repair, in this contribution, a hybrid of multi-frequency phase and code measurement is applied to eliminate the ambiguity term after fixing cycle slip to get continuous arcs according to Eq. (1).

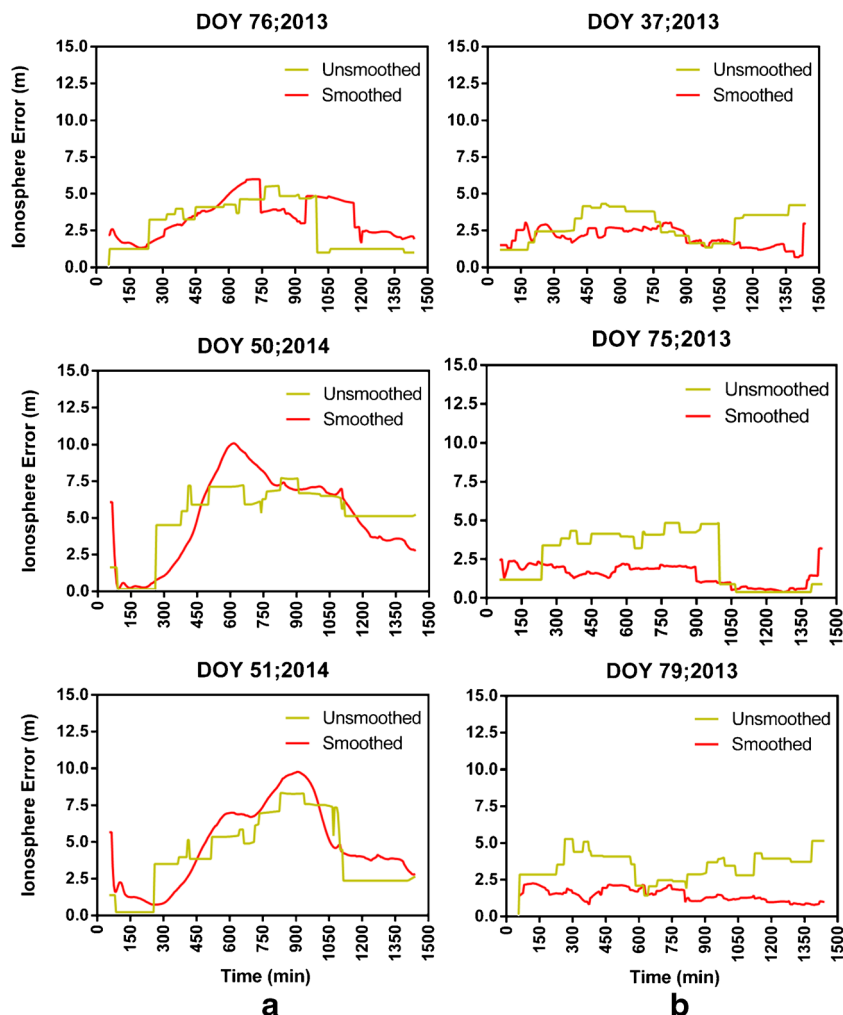
- 2 Estimating the average between phase and code for continuous arcs. The ionospheric effects are canceled, and biases are introduced as follows (e.g., Xiang et al. 2017):

$$L_{GF} = L_1 - L_2 = (1 - \gamma)I + B_1 + DPB_{\phi_1 - \phi_2}^s - DPB_{\phi_1 - \phi_2}^r + \epsilon_\phi \tag{4}$$

$$P_{GF} = P_2 - P_1 = (1 - \gamma)I + DCB_{P_1 - P_2}^s - DCB_{P_1 - P_2}^r + \epsilon_P \tag{5}$$

where L_{GF} and P_{GF} are the phase and code measurement geometry free, I is the L_1 ionosphere blunder at GPS receiver location, γ is the factor to convert the ionospheric delay from L_1 to L_2 frequency, $B_I = \lambda_1 N_1 - \lambda_2 N_2$ is the ionosphere ambiguity variable, DPB is the differential phase biases (where subscription s for satellite and r for the receiver), DCB is the differential code biases (where subscription s for satellite and r for the receiver), ϵ_ϕ , ϵ_P other unmodeled errors in phase and code measurement.

Fig. 6 Errors caused by the ionosphere at MANS GPS station during stormy days (a) and quiet days (b)



$$\begin{aligned}
 (L_4 - P_4)_{\text{arc}} &= \frac{1}{n} \sum_1^n (L_4 - P_4)_i \\
 &= (B_I + \text{DPB}_{\phi_1 - \phi_2}^s - \text{DPB}_{\phi_1 - \phi_2}^r) - \text{DCB}_{P_1 - P_2}^s \\
 &\quad + \text{DCB}_{P_1 - P_2}^r + (\varepsilon_P)_{\text{arc}}
 \end{aligned}
 \tag{6}$$

3- Eliminating ambiguity term as follows:

$$\begin{aligned}
 L_{\text{smoothed}} = L_4 - (L_4 - P_4)_{\text{arc}} &= (1 - \gamma) \text{MF}(I) \\
 &\quad + (\text{DCB}_{P_1 - P_2}^s - \text{DCB}_{P_1 - P_2}^r) \\
 &\quad + (\varepsilon_P) + \varepsilon_L
 \end{aligned}
 \tag{7}$$

In this model, $\text{DCB}_{P_1 - P_2}^r$ and $\text{DCB}_{P_1 - P_2}^s$ are estimated using the zero difference DCB estimation (ZDDCBE) code published by Sedeek et al. (2017)

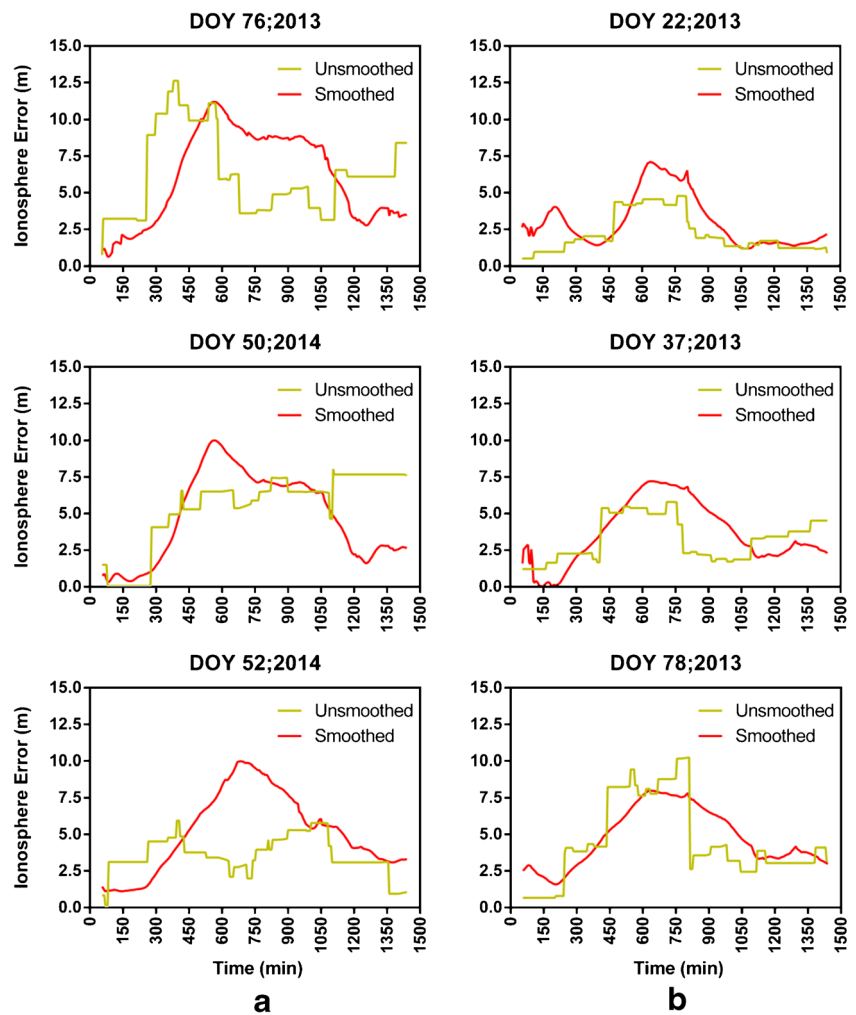
The main advantages of a smooth code can be seen in reducing noise and in avoiding the direct resolution of ambiguities. However, the biggest challenge is to level errors.

Mapping function (MF) is used as a basis of a spherical ionosphere single layer model, which is computed according to, e.g., Leandro et al. (2010):

$$\text{MF} = \sqrt{1 - \left(\left(\frac{r}{r + sh} \right) \cos(e) \right)^2}
 \tag{8}$$

where r is the radius of Earth, h is the ionosphere shell height, β is the angle of elevation of the satellite at the shell

Fig. 7 Errors caused by the ionosphere at MTRH GPS station during stormy days (a) and quiet days (b)



height piercing point, and e is the elevation angle of the satellite at receiver as seen in Fig. 1.

The ionosphere blunder estimation is executed using SLSA expressed as (Xu 2007)

$$L = AX \tag{9}$$

$$X = (A_1^T \times W_1 \times A_1 + A_2^T \times W_2 \times A_2)^{-1} (A_1^T \times W_1 \times l_1 + A_2^T \times W_2 \times l_2) \tag{10}$$

where A_1 and A_2 are the design matrix of the first and the second groups of observations, respectively, W_1 and W_2 are the weight matrices of the first and the second groups of observations, respectively, l_1 and l_2 are the observation vectors of the first and the second group, respectively, and X is the anonymous parameter vector.

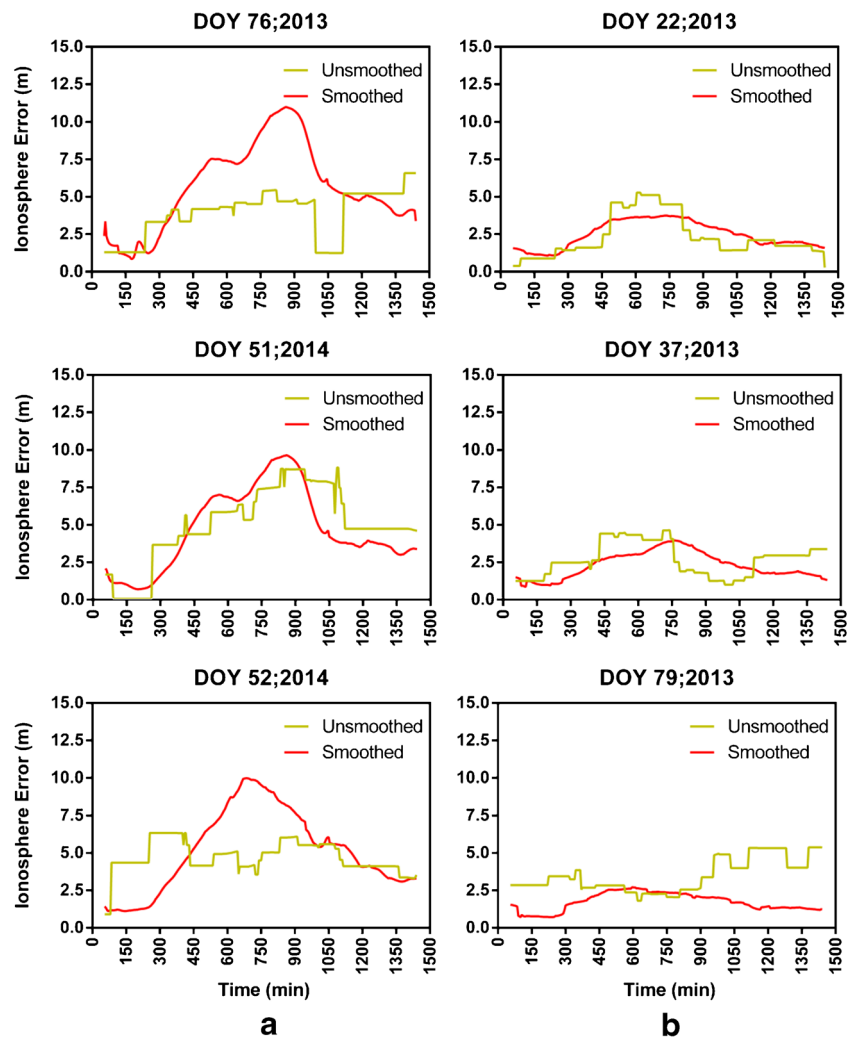
These models were handled in MATLAB® and were named IEE. Figure 2 demonstrates the block diagram of the ionosphere error computation using the IEE program.

Case study

In this contribution, Kp , Ap indices, and the G-scale were utilized to investigate the origins and effects of the worldwide magnetic activity. The planetary K -index is taken into account as a superb indication for irregularities within the magnetic field of the Earth. It varies between 0 and 9, where a value of 0 is minimal, and 9 indicates a severe geomagnetic storm. The National Oceanic and Atmospheric Administration (NOAA) uses a five-level G-scale to denote the intensity of the geomagnetic activity detected and predicted. This scale varies from G0 to G5; G0 is the lowest and G5 the highest (Du et al. 2010). G-level and its correspondence K_p value appear in Table 1.

In this contribution, the IEE program was applied to compute the ionosphere blunder using smoothed and unsmoothed phase observables for six ground-based multi-frequency GPS receivers, using observations based on days of quiet conditions (no geomagnetic storms). These stations, which are lo-

Fig. 8 Errors caused by the ionosphere at SAID GPS station during stormy days (a) and quiet days (b)



cated over Egypt, are called Marsa-ALAM, ASWAN, BORG-ELARAB, MANSOURA, MATROUH, and PORT-SAID, as appeared in Fig. 3. Then, the IEE program was applied again on the same six stations using observations based on days with high geomagnetic storms.

Quiet and stormy days in this investigation were indicated using tesis.lebedev.ru/, which presents the values of K_p , A_p indices, and G-scale that are given in Table 2.

To investigate the influence of the geomagnetic storms on ionosphere blunder, the consequences of stormy and quiet days compared. The next figures (Figs. 4, 5, 6, 7, 8, and 9) show the estimated ionosphere blunder values of the stations, using smoothed and unsmoothed phase observations, in various geomagnetic conditions and the distinction between them. These differences describe the influence of the geomagnetic storms on ionosphere blunder.

Results

The influence of geomagnetic storms on the computed ionosphere can be noted after using the IEE program on the stations mentioned above. Figures 4, 5, 6, 7, 8, and 9 show a comparison between the estimated ionosphere blunder using smoothed and unsmoothed phase observables during various geomagnetic conditions, according to indices of K_p , A_p , and G-scale, which were provided by tesis.lebedev.ru/. Each figure of them describes the ability of geomagnetic storms in disturbing the computed ionosphere blunder.

Table 3 shows mean ionosphere error (MIE) and standard deviation of mean (SDM) for several DOY through stormy and quiet days using unsmoothed and smoothed phase observation, where the red text is the highest value and the blue one

Fig. 9 Errors caused by the ionosphere at ASWN GPS station during stormy days (a) and quiet days (b)

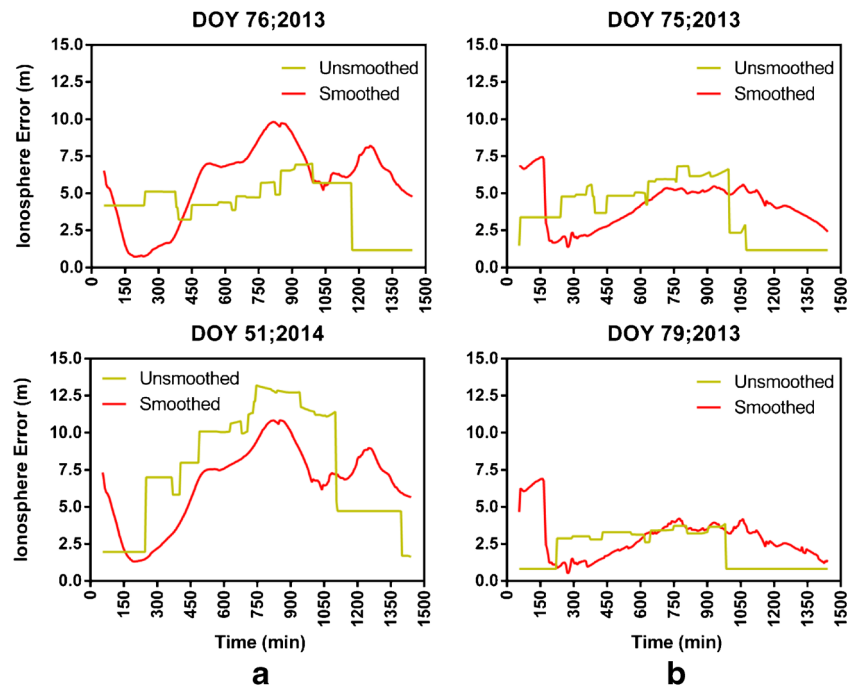
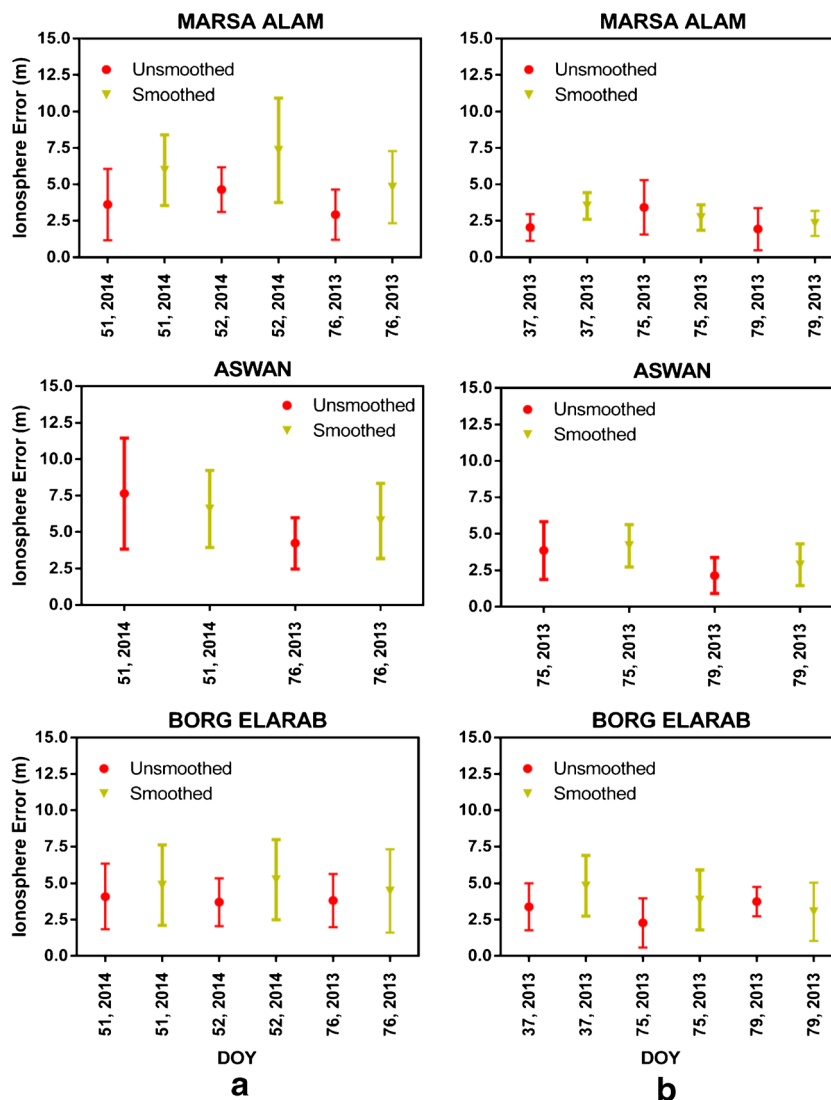


Table 3 The estimated mean ionosphere error and standard deviation of the mean for GPS stations over Egypt using observations based on days of stormy and quiet conditions

Receivers	Stormy					Quiet				
	DOY	Unsmoothed		Smoothed		DOY	Unsmoothed		Smoothed	
		AVG (m)	SDM (m)	AVG (m)	SDM (m)		AVG (m)	SDM (m)	AVG (m)	SDM (m)
MARSA ALAM (ALAM)	51, 2014	3.61	0.15	5.99	0.14	37, 2013	2.04	0.06	3.53	0.05
	52, 2014	4.65	0.09	6.62	0.21	75, 2013	3.42	0.11	2.73	0.05
	76, 2013	2.92	0.10	4.85	0.14	79, 2013	1.93	0.09	2.34	0.05
ASWAN (ASWN)	51, 2014	7.64	0.23	6.62	0.15	75, 2013	3.85	0.12	4.27	0.09
	76, 2013	4.23	0.11	5.80	0.15	79, 2013	2.15	0.07	2.95	0.09
BORG EL-ARAB (BORG)	51, 2014	4.09	0.13	4.79	0.16	37, 2013	3.39	0.10	4.78	0.12
	52, 2014	3.70	0.10	5.17	0.16	75, 2013	2.28	0.10	3.84	0.13
	76, 2013	3.82	0.11	4.33	0.17	79, 2013	3.75	0.06	3.02	0.16
MANSOURA (MANS)	50, 2014	5.17	0.13	5.01	0.17	37, 2013	2.86	0.06	2.03	0.04
	51, 2014	4.20	0.15	4.74	0.16	75, 2013	2.56	0.10	1.50	0.05
	76, 2013	2.88	0.10	3.38	0.08	79, 2013	3.47	0.05	1.46	0.03
MATROUH (MTRH)	50, 2014	5.46	0.15	4.71	0.18	22, 2013	2.18	0.08	3.03	0.10
	52, 2014	3.59	0.08	5.17	0.16	37, 2013	3.26	0.09	3.64	0.13
	76, 2013	6.20	0.17	6.13	0.19	78, 2013	4.50	0.17	4.75	0.12
PORT SAID (SAID)	51, 2014	5.01	0.15	4.68	0.16	22, 2013	2.33	0.08	2.50	0.05
	52, 2014	4.73	0.06	5.05	0.16	37, 2013	2.68	0.07	2.31	0.05
	76, 2013	3.89	0.09	5.63	0.17	79, 2013	3.47	0.07	1.71	0.04

Fig. 10 Mean ionosphere error and standard deviations at ALAM, ASWN, and BORG GPS stations for stormy days (a) and quiet days (b)



is the lowest value at each station. The consequences of the mean and standard deviations of the mean for estimated ionosphere error throughout days of stormy conditions extend between 23 (at ASWN) and 6 cm (at SAID) using the unsmoothed phase model and between 21 (at ALAM) and 8 cm (at MANS) using the smoothed phase model. Otherwise, the SDM for the estimated ionosphere error throughout quiet conditions extends between 17 (at MTRH) and 5 cm (at MANS) using the unsmoothed phase model and between 16 (at BORG) and 3 cm (MANS) at using the smoothed phase model.

As shown in Figs. 4, 5, 6, 7, 8, and 9, eliminating ambiguity term using the smoothed phase model provides results much smoother than unsmoothed phase results. I think this is because of the fixed ambiguity

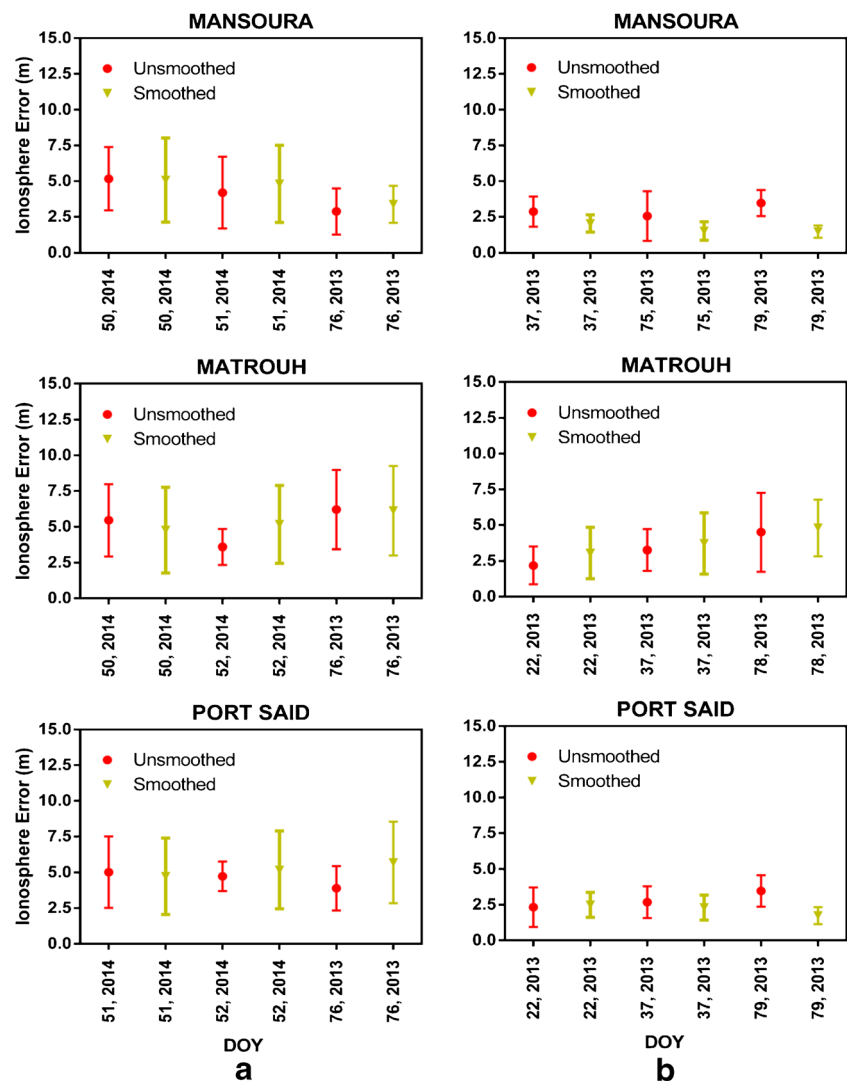
over the continuous arc, as solar flare increases in mid of the day the ionosphere error increase.

Geomagnetic activity plays an essential role in disturbing the ionospheric blunders. The highest estimated ionospheric error using the unsmoothed model is 13.19 m in a stormy day at low latitude station (ASWN) (see Fig. 9a) (DOY51; 2014), and the highest estimated ionospheric error using the smoothed model is 13.34 m in a stormy day at low latitude station (ALAM) (see Fig. 4a) (DOY52; 2014).

Figures 10 and 11 show mean ionosphere errors and the standard deviations (SD) for stormy and quiet day of year (DOY) estimated by the proposed models.

From analyzing the results of two models, a relatively high MIE and SD over six GPS stations can be noticed in stormy

Fig. 11 Mean ionosphere error and standard deviations at MANS, MTRH, and SAID GPS stations for stormy days (a) and quiet days (b)



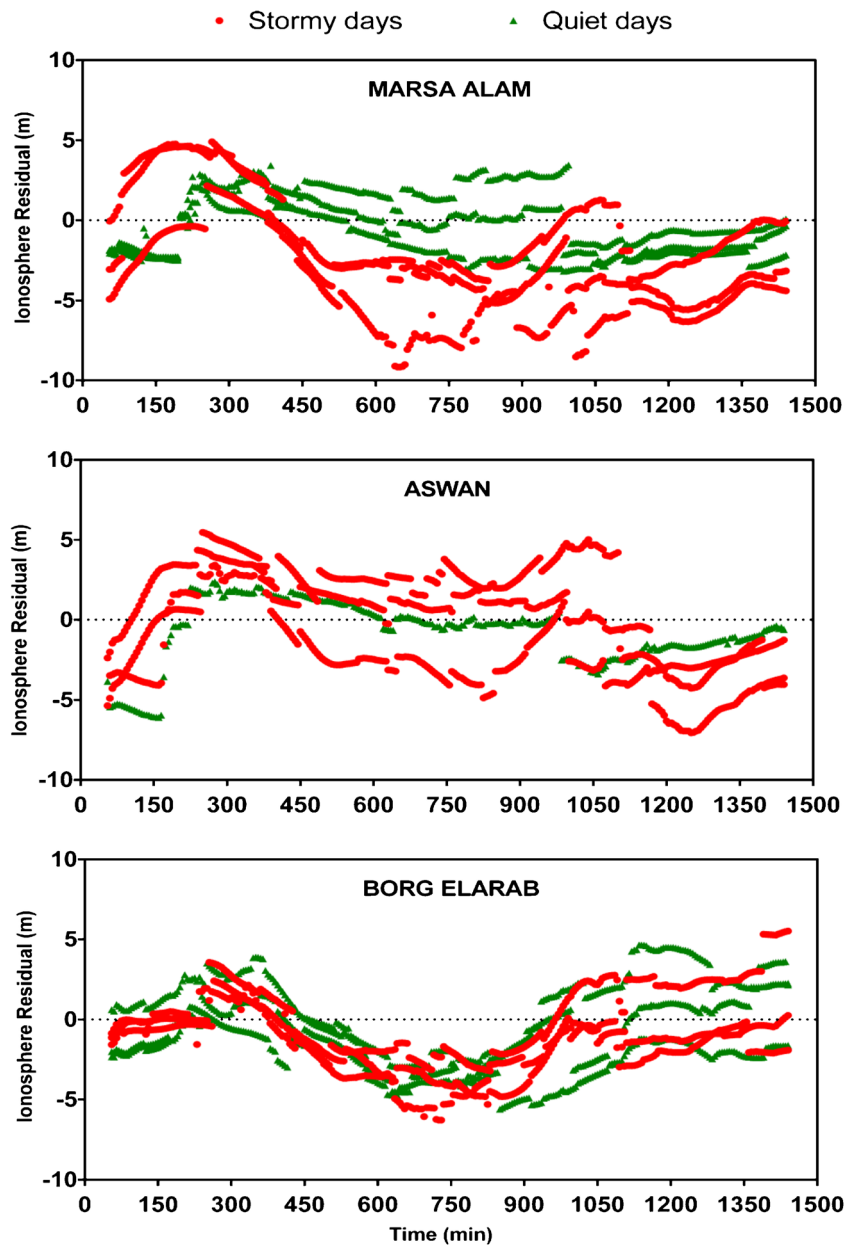
days (see Figs. 10a and 11a) and a significant decrease in MIE and SD in quiet days (see Figs. 10b and 11b).

The ionospheric error residuals are the difference between the ionospheric error from unsmoothed and smoothed phase observables. Figures 12 and 13 demonstrate the ionosphere error residuals at each GPS receivers over Egypt for 3 quiet days and 3 stormy days, except Aswan ionosphere error residuals for 2 quiet days and 2 stormy days. As seen in Figs. 12 and 13, geomagnetic activity has a significant effect on estimating ionospheric blunders. The highest residual was 9.15 m at a low latitude location (ALAM) in stormy condition, and the minimal residual was 0.84 m at SAID station in the quiet condition. The higher ionospheric error ranges observed at three GPS stations (ALAM (low latitude), ASWN (low latitude), and

MANS (mid-latitude)) all were in stormy days, while the lower ranges (ALAM (low latitude), SAID (Mid-latitude), and MANS (Mid-latitude)) all were in quiet days.

Also, residuals around the mean were estimated for both models; the maximum and minimal difference using the unsmoothed phase model was 13 m at ASWN station in a stormy day and 1.02 m at SAID station in a quiet day, respectively. While the maximum and minimal differences using the smoothed phase model were 6 m at ALAM station in a stormy condition and 0.67 m at MANS station in a stormy condition, respectively. The smoothed phase observables demonstrate the lowest difference around the mean in the stormy and quiet days. The summary of these investigations explained in the conclusion.

Fig. 12 Ionosphere residuals over three GPS stations (ALAM, ASWN, BORG) for stormy and quiet days



Conclusions

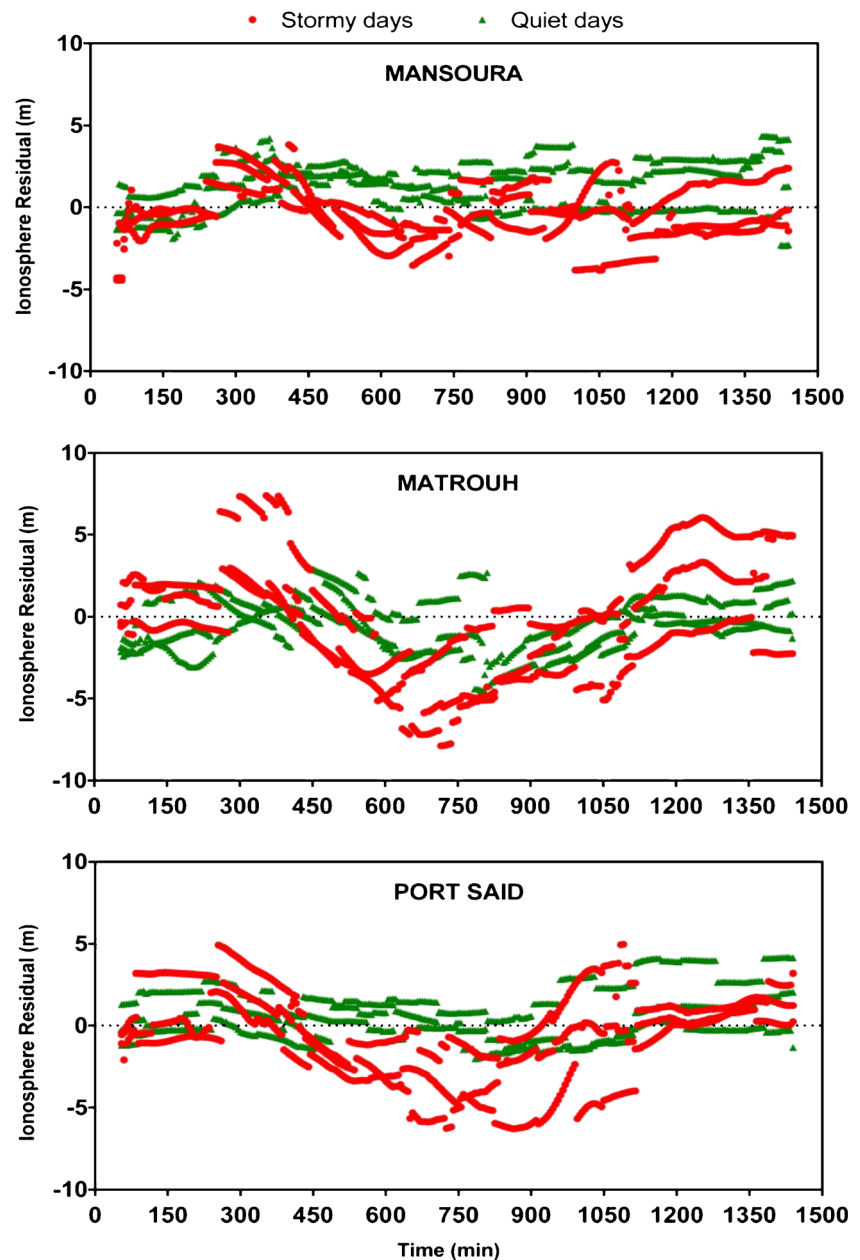
In this paper, the ionospheric delay acquired from fixing ambiguity using a linear combination of pseudo-range and phase observables (unsmoothed phase) and carrier phase smoothed code method (smoothed phase) to avoid addressing ambiguity bias directly. After result analysis, these conclusions can be derived:

- the ionospheric blunders from the smoothed phase model much smoother compared with the unsmoothed phase

model, due to eliminating ambiguity term by smoothing phase observation.

- The ionosphere blunder relies upon the magnetic activity as the error increases with the increase of K_p and A_p indices.
- The geomagnetic storms increased the estimated ionospheric error using the unsmoothed and smoothed phase model by about 200% as in ASWN and by about 265% as in SAID, respectively.
- The geomagnetic storms increase the SDM of the estimated ionospheric error using the unsmoothed and smoothed

Fig. 13 Ionosphere residuals of three GPS stations (MANS, MTRH, SAID) for stormy and quiet days



phase model by about 180% as in MANS and by about 350% as in SAID, respectively.

- Ionosphere error relies upon the station latitude where the ionospheric error increases and can be a real problem in equatorial and high-latitude regions as ASWAN and ALAM stations.

Finally, the contrast between the stormy and quiet ionosphere errors clarifies the necessity of estimating the ionosphere blunders when considering GPS observations to

improve the precision of point positioning, especially throughout stormy days. For further works, using other modes for fixing ambiguity, and converting the estimated ionosphere bias from smoothed and unsmoothed phase models into VTEC and investigating its effect on point positioning.

Acknowledgments Crustal Dynamics Data Information System (CDDIS) is acknowledged for providing DCB, SP3, IONEX files. The author was also grateful to worthy comments and recommendations from anonymous referees.

References

- http://tesis.lebedev.ru/en/magnetic_storms.html. Accessed 15 Feb 2020
- <https://www.noaa.gov/>. Accessed 15 Feb 2020
- Bhattacharya S, Dubey S, Tiwari R, Purohit PK, Gwal AK (2008) Effect of magnetic activity on ionospheric time delay at low latitude. *J Astrophys Astron*. <https://doi.org/10.1007/s12036-008-0035-9>
- Dengynu L, Weijun L, Xiaoxin C, Dunshan Y (2012) Carrier-aided smoothing for real time Beidou positioning, Proceedings of the 2012 International Conference on Information Technology and Software Engineering, Beijing, China, 8–10 Dec
- Du D, Xu WY, Zhao MX, Chen B, Lu JY, Yang GL (2010) A sensitive geomagnetic activity index for space weather operation. *Space Weather Int J Res Appl*. <https://doi.org/10.1029/2010SW000609>
- Elghazouly AA, Doma MI, Sedeek AA, Rabah MR, Hamama MA (2019a) Validation of global TEC mapping model based on spherical harmonic expansion towards TEC mapping over Egypt from a regional GPS network. *Am J Geogr Inf Syst* 8(2):89–95. <https://doi.org/10.5923/j.ajgis.20190802.04>
- Elghazouly AA, Doma MI, Sedeek AA (2019b) Estimating satellite and receiver differential code bias using a relative Global Positioning System network. *Ann Geophys* 37(1039–1047):2019. <https://doi.org/10.5194/angeo-37-1039-2019>
- Elsayed A, Sedeek A, Doma M, Rabah M (2018) Vertical ionospheric delay estimation for single-receiver operation. *J Appl Geodesy*. <https://doi.org/10.1515/jag-2018-0041>
- Ghilani CD, Wolf PR (2014) Elementary surveying, 14th edn. Pearson. ISBN: 978-0-13-375888-7
- Hofmann-Wellenhof B, Lichtenegger H, Wasle E (2008) GNSS – global navigation satellite systems – GPS, GLONASS, Galileo & more. Springer-Verlag, Wien
- Klobuchar JA (1991) Ionospheric effects on GPS. *GPS World* 4:48–51
- Leandro RF, Santos MC, Langley RB (2010) Analyzing GNSS data in precise point positioning software. *GPS Solutions* 15(1):1–13. <https://doi.org/10.1007/s10291-010-0173-9>
- Sedeek AA, Doma MI, Rabah M, Hamama MA (2017) Determination of zero difference GPS differential code biases for satellites and prominent receiver types. *Arab J Geosci* 10
- Sickle JV (2015) GPS for land surveyors, 4th edn. CRC Press. ISBN: 9781-4665-8311-5
- Sidorov R, Soloviev A, Gvishiani A, Getmanov V, Mandea M, Petrukhin A, Yashin I, Obratsov A (2019) A combined analysis of geomagnetic data and cosmic ray secondaries for the September 2017 space weather event studies. *Russ J Earth Sci* 19:1–10. <https://doi.org/10.2205/2019ES000671>
- Xiang Y, Gao Y, Shi J, Xu C (2017) Carrier phase-based ionospheric observables using PPP models. *J Geodesy Geodyn* 8(1):17–23. <https://doi.org/10.1016/j.geog.2017.01.006>
- Xu G (2007) GPS theory, algorithms and applications, Library of Congress Control Number: 2007929855. ISBN second edition 978-3-540-72714-9. Springer Berlin Heidelberg, New York
- Leandro, R. F. (2009) Precise Point Positioning With GPS A New Approach For Positioning, Atmospheric Studies, And Signal. PhD Thesis, University of New Brunswick